Bolted Connections of Pultruded GFRP: Implications of Geometric Characteristics on Net Section Failure

Ana M. Girão Coelho

Marie Curie IEF Research Fellow
(corresponding author, a.m.girao-coelho@warwick.ac.uk)
Civil Research Group, School of Engineering, University of Warwick
Coventry CV4 7AL, UK

J. Toby Mottram

Professor
(j.t.mottram@warwick.ac.uk)
Civil Research Group, School of Engineering, University of Warwick
Coventry CV4 7AL, UK

Kent A. Harries

Associate Professor
(kharries@pitt.edu)
Department of Civil and Environmental Engineering, Swanson School of Engineering,
University of Pittsburgh, Pittsburgh PA 15261, USA

Abstract. The results of a three-dimensional finite element study of the net section dominated failure behaviour of pultruded open-hole specimens are presented. Computer models are developed using the general-purpose software Abaqus. Several issues are addressed in the study with respect to the notched plate geometry: (i) thickness of plate, (ii) transverse centre-to-centre spacing of holes (gauge), and (iii) distance from the centre of the hole to the nearest edge. The analytical results provide information on basic performance and the effects of these parameters on strength and damage tolerance performance, thereby furthering the current understanding of pultruded plate-to-plate connection behaviour under static loading. Based on the results, design recommendations for minimum edge distance and gauge spacing for bolts are given.

Keywords. Damage mechanics; Fibre-tension failure; Finite element modelling; Geometry requirements; Open-hole tensile test; Pultruded material.

1. Introduction

Due to a range of advantages associated with the high specific strength and stiffness, durability, thermal properties and durability of pultruded Glass Fibre Reinforced Polymer (GFRP) composites, these materials are becoming recognised as an attractive alternative primary structural material in low-rise building residential and commercial construction. The likely extensive use of off-site prefabrication utilizing these light-weight materials requires on-site connections for components that ensure strength, stiffness and ductility while remaining simple to fabricate. This argues for the use of mechanical fasteners and a limited number of simple components. A comprehensive review of the research work carried on bolted connections of pultruded GFRP for main structural components in buildings has been reported in [1].

Plate-to-plate bolted shear connections are the primary connection type for pultruded GFRP material because they are familiar and easy to use. Their load transfer is made by plates in bearing and bolts in shear. The mechanical behaviour of this type of connection triggers the bolt shear, the bolt-hole bearing and the net section deformation. The ultimate load carrying capacity of the connection will be governed by one of many failure modes including bearing, end pull-out, net section fracture, bolt shear, block shear rupture, etc. Typically, net section fracture is critical in connections with relatively narrow plate widths. However, if (well designed) connections are allowed to rupture, failure will eventually occur by net tension preceded or not by localized bearing distortion. Therefore, it is not feasible to provide a theoretical minimum value for the plate width. Any value could be specified.

In 2010, the American Society of Civil Engineers submitted the Pre-Standard for Load & Resistance Factor Design of Pultruded Reinforced Polymer Structures [2] (ASCE pre-standard, hereafter) to the American Composites Manufacturers Association so that it could be transferred to the ASCE/SEI Standards Committee for officially processing as a formal ASCE standard. This pre-standard has an individual chapter on the *Design of bolted connections* that provides guidance on the strength design of *bearing type* bolted connections for pultruded GFRP shapes. Related minimum geometry dimensions tied to the diameter d of the steel bolting are given possibly to facilitate construction, and essentially follow the rules given in the 1960 Marine Design Manual for Fibreglass Reinforced Plastics [3], with some limited modifications (see Fig. 1 and Table 1). To the best knowledge of the authors, there is no previous research pertaining to the implications of such minimum requirements on the strengths of plate-to-plate shear connections.

In order to verify or improve the design rules for connections of pultruded GFRP, a computational study into the response to failure of pultruded flat sheets with through-thickness holes subjected to in-plane tension is conducted. The parametric study focuses on connections with

a single row of one or two bolts in a double-lap shear configuration, so that the flexural deformation of the plate is not relevant. Virtual tests for the stress and failure analysis of open hole pultruded composite plates subjected to increasing in-plane tension load are carried to serve as a convenient framework for the interpretation of test data on the composite load-bearing capacity [4,5]. The three-dimensional finite element representations of such structural systems have been developed by Girão Coelho *et al*. [6], and validated against existing test results from recent experiments conducted at the University of Pittsburgh [7]. The numerical models are based on critical stress combinations that trigger damage initiation, and critical energy release rates that describe damage propagation to ultimate failure. They are used in this work to perform parametric studies of the geometry of these open hole tension specimens, including edge (or side) distance e_2, gauge p_2 (i.e. hole-to-hole spacing across the width), and hole diameter d_0. In Table 1 the second and third columns list the minimum requirements for these three geometric parameters taken from the ASCE pre-standard for pultruded materials and for structural grades of steel in accordance with EN 1993-1-8 [8].

By studying the fibre-tension dominated progressive failure process across the net-tension plane, the connection geometry is discussed in detail, and recommendations for the design purpose are made based on the following performance requirements for static loading: *tensile stress* (i.e. the applied load averaged over the nominal gross cross-section) and *damage tolerance*, which is quantified below by means of a *resistance index* R_{FRP}, defined as the ratio of the stress level corresponding to full damage to the plate side edges σ_{Fd} and unnotched strength σ_{max}.

2. Fundamental behaviour and analysis approach

The physical characteristics that can influence the tensile behaviour of bolted plate-to-plate connections of pultruded material include:

- the through-thickness hole diameter d_0,
- the plate thickness t,
- the number and arrangement of bolts,
- the connection geometry, more specifically the end and edge distances, e_1 and e_2, the pitch p_1 and the gauge p_2 of bolts (see Fig. 1).

The limitations on edge distance and spacing of bolts that should be adhered to in connections are imposed (i) to facilitate construction and (ii) to satisfy the requirements for strength and damage

tolerance. The minimum dimensions can be established by studying the net tension rupture mechanism of a bolted connection that gauges the connection load bearing capacity.

The net section failure mode of a bolted connection is assumed to be identical to tensile fracture of a plate with unfilled through-thickness holes. The Open Hole Tensile (OHT) test is representative of the behaviour of composite components with fastener hole (which is not unreasonable given that the plate material fracture – fibre breakage – is well known to occur under tensile loading). It thus allows for prediction of the strength in the net section failure mode for use in design of bolted connections.

The existence of holes in a plate causes a geometrical discontinuity and a disruption of the stress field, and, as a consequence, stress concentrations occur in the region of the hole(s). The magnitude of the stresses increases with the applied load until fracture initiates at the edge of the bolt hole, where the maximum stress concentration develops. These high values of stress in the vicinity of the hole cause damage during loading prior to ultimate failure. A salient feature of the deformation of OHT in net section rupture is the rapid propagation of the internal damage either to the nearest side edge or, when there are two of more holes in a row, between two holes. This is a typically brittle type fracture that is characteristic of composites reinforced with continuous fibres, except when subjected to shear.

A continuum shell finite element approach and progressive damage analysis are chosen in this work as being both necessary and sufficient for modelling of the above behaviour. Increment-iterative solution procedures are applied to capture the combined geometric and material nonlinear effects on the response of OHT specimens representing connection plate design. Only pultruded plates containing symmetrically stacked layers of E-glass unidirectional rovings and continuous filament mats in a polyester resin are considered in the parametric studies. For modelling purposes however, the plate is considered as a homogeneous continuum, i.e. the material is homogenized by smearing the behaviour of the fibres and the matrix over a single lamina. It is of relevance to this contribution to understand that the composite architecture typically found in pultruded GFRP shapes plates ensures that delamination is unlikely to occur under tension. Unnotched flat sheet (plate) material was characterized for the moduli of elasticity in the pultruded (or unidirectional fibre) and transverse direction, E_1 and E_2, and axial strength of the plate material in tension and transverse strength in tension, $f_{1,T}$ and $f_{2,T}$, see Table 2 [6]. The mechanical behaviour of a lamina in a progressive failure modelling approach is further characterized by the fracture toughness $G_{1,T,c}$ in axial and $G_{2,T,c}$ in transverse directions (Table 2). Guidelines for the evaluation of these progressive failure properties can be found in [9,10]. Boundary conditions consistent with the geometric symmetry of the OTH rectangular plate model illustrated in Fig. 2 are employed but not in the pultrusion direction, as the conditions restraining movement may change the stress field.

A comprehensive summary of the subject area of numerical modelling of bolted composite connections of composite material and the details of our finite element modelling and validation are given in [6]. The analyses are conducted using the software Abaqus [11]. The continuum damage model implemented in Abaqus predicts the onset and accumulation of intralaminar damage mechanisms (in the form fibre breakage, in this specific case), as well as final structural collapse by the propagation of a macro-crack. For this modelling, the Hashin criterion [12] is used for damage initiation. The fibre tension damage progression is tracked, from 0 to 1, using the Abaqus option DAMAGEFT. The influence of damage on the constitutive model is based on the work of Matzenmiller *et al*. [13]. A drawback of this damage progression model is that it does not reproduce localization of the tensile fracture properly. This aspect is resolved by means of the crack band approach formulated by Bažant and Oh [14]. The crack band model uses a modification of the post-peak part of the constitutive law (damage progression) to enforce the energy dissipation as observed in experiments by a localized crack band that occurs along the centre of the notched cross-section.

3. Virtual test configurations and parameters

The generic configuration for the finite element virtual tests performed in this research is shown in Fig. 2. All simulations are conducted using the material properties from Table 2. Specific characteristics and attributes modelled in all these studies are as follows:

- all tests involve in-plane uniform tension applied at a distance $4d_0$ from the net-tension failure plane to simulate the behaviour of plates of constant width and thickness with through-thickness holes,
- the plates contain a single row of (equal) diameter hole(s),
- a plate thickness of 6.4 mm (¼ in.) is assumed in all the studies,
- the end distance e_1 for the bolting is kept constant at $4d_0$; thus the length of the plate is varied for each virtual test,
- in-plane modelling parameters such as element size and shape are kept constant in the finite element models, irrespective of hole size, to predict failure loads and failure progression.

Variables considered in the parametric studies are (see Table 3):

- hole diameter d_0,
- ratio of thickness-to-hole diameter t/d_0,
- ratio of gauge for the bolting-to-hole diameter p_2/d_0,

- ratio of edge distance-to-hole diameter e_2/d_0.

These are varied parametrically as shown in Table 3. Specific values of the above variables and considered within the parametric studies are given in Tables 4 and 5 (w: section width) in Section 4. The OTH configurations are divided into two series each focusing on a different geometric parameter. All simulations are conducted using the material properties from Table 2. The main variable in series $E2$ is the edge distance e_2, which has a significant effect on the mode of failure of plate-to-plate connections. Series $P2$ is centred on the effect of the distance between bolt hole centrelines p_2 (gauge). The decision process in retaining certain values for the above ratios and eliminating the need to consider certain combinations of configuration variables was supported by previous experimental data summarized in [1] and also by the fact that research results most pertinent to the present study are those for values near or above the limits given for the ratio e_2/d_0 and near or below the limits given for p_2/d_0. The configurations in Tables 4 and 5 are labelled according to the system $S\_e_1/d_0\text{-}e_2/d_0\text{-}p_1/d_0\text{-}p_2/d_0\text{-}t/\ d_0$ (where S is for the series, $E2$ or $P2$).

One final remark on the chosen configurations concerns the choice of the hole diameter d_0 parameter to be varied instead of the bolt diameter d as currently assumed in the ASCE pre-standard. This option has the advantage of harmonizing the pre-standard provisions with current European design code for steel joints [8].

4. Analysis results

Figures 3-8 and Tables 4 and 5 summarize the strength and damage results from all the parametric studies. In the graphs, the *strength reduction factor k*, defined as the ratio of the maximum predicted tensile stress to the unnotched strength is plotted against the relevant variable. Only the portion of the curves for $0.5 < k < 0.8$ is shown in Figs. 4 and 7 to increase the resolution of the plots. The fibre-tension damage contour plots for two selected plate configurations are shown in Figs. 5 and 8. The two tables set out the numerical tests that have been conducted, the sequencing of these tests and the corresponding performance indicators, strength and resistance index.

4.1. Effect of edge distance: series E2

The relationship between edge distance to hole diameter ratio and the strength reduction factor computed from the finite element simulations are plotted in Figs. 3 and 4. It can be seen from these plots that there is hardly any sensitivity to the hole diameter. This is an expected outcome as the

specimens are sized with respect to changing d_0, so that the results are independent of the size of the hole (see also Table 4).

The numerical predictions show an increase of the (notched) plate strength with the edge distance ratio. The results indicate that the response can be approximated by a quadratic function, $k = -0.05(e_2/d_0)^2 + 0.33e_2/d_0 + 0.20$ (solid line in the plot of Fig. 4), with an R-squared value of 0.98. Since the k value for $e_2/d_0 = 1.2$, which corresponds to the minimum value for the design of metallic joints [8], is much lower ($k = 0.51$), the corresponding results are not considered for further comparisons. The k factor is improved by about 27% by changing e_2/d_0 from 1.5 (which is the current minimum value specified in the ASCE pre-standard) to 3.0. However, when e_2/d_0 is decreased from 3.0 to 2.5, the differences in the strength reduction factor are much smaller (2.7%). This result suggests that the recommended limit for the ratio e_2/d_0 in the ASCE pre-standard does not consistently develop the desired strength level and should be revised upward to at least $e_2/d_0 \geq 2.5$.

The fibre-tension damage contour plots for specimen E2_4.0-2.5-0-0-1/2 (with $e_2/d_0 = 2.5$) are shown in Fig. 5 for two different stress levels. The DAMAGEFT distributions are shown for the stress level corresponding at full net section damage (Fig. 5a) and at collapse (Fig. 5b).

4.2. Effect of gauge spacing: series P2

Figures 6 and 7 illustrate the effect of varying the ratio p_2/d_0 with the strength reduction factor for different ratios of the plate thickness. In both plots, the black markers/line correspond to the current $e_2/d_0 = 1.5$ proposed in the ASCE pre-standard. The grey markers/line are for $e_2/d_0 = 2.5$, which has been shown to be a more acceptable geometric limit to comply with the adopted performance parameters. The plots again show little or no sensitivity to changing the hole diameter. The two solid lines in Fig. 7 correspond to the regression data analysis and correspond to a quadratic approximation ($k = -0.03(p_2/d_0)^2 + 0.06p_2/d_0 + 0.40$, for $e_2/d_0 = 1.5$ and $k = -0.01(p_2/d_0)^2 + 0.10p_2/d_0 + 0.43$, for $e_2/d_0 = 2.5$), which was found to provide the best fit.

It is clear from the two plots (and from the numerical results in Table 5 as well) that the strength predictions with $e_2/d_0 = 1.5$ are always lower than those with $e_2/d_0 = 2.5$, except for the case of $p_2/d_0 = 1.5$, which is in fact an unrealistic ratio to choose. Therefore, only the results for the edge ratio of 2.5 are retained for further analysis.

The notched plate strength increases steadily as p_2/d_0 is increased until $p_2/d_0 = 4.0$. For this ratio, the curve virtually levels off with $k \approx 0.70$. If we take $p_2/d_0 = 4.0$ as a reference (which is a reasonable assumption as it corresponds to the ASCE pre-standard requirement limit), k decreases

by 2.2% when $p_2/d_0 = 3.5$ and by 5.1% when $p_2/d_0 = 3.0$. It can be argued that the current limit provides a conservative estimate of the ultimate tensile strength of notched plates.

Finally, Fig. 8 shows the DAMAGEFT contours for specimen P2_4.0-2.5-0-3.0-1/2 (with $e_2/d_0 = 2.5$ and $p_2/d_0 = 3.0$) for the identical stress levels of the previous section. The damage zone propagates across the material between the pair of holes (as well as towards the free edge), indicating an interaction between the two holes.

5. Practical implications

The finite element analyses reported shed light on the effects of the geometric characteristics on the net section failure potential. The following are general observations regarding the effects of edge distance e_2 and gauge p_2:

1. Notched plates with smaller edge distance to hole diameter ratios are expected to have a lower tensile strength. Analysis of the data shows that the requirements for the recommended minimum ratio e_2/d_0 have to be tighter than those currently proposed in the ASCE pre-standard. The authors suggest that a minimum value of $e_2/d_0 = 2.5$ should be adopted in practice.
2. The simulation results suggest that there is a limit for the gauge to hole diameter ratio from which the increase in the plate tensile strength is insignificant. The authors have estimated this limit to be in the neighbourhood of $p_2/d_0 = 3.0$.
3. Plate configurations for the specific groups of tests have been equally sized to the hole diameter. The results of the simulation studies conducted show that the structural behaviour is not influenced by the thickness of plate to hole diameter ratio.
4. The potential for a brittle net section failure (i.e. high values of the resistance index R_{FRP}, say ≥ 0.90) is independent of the connection geometric characteristics scoped in the study.

The numerical data provides support for revisiting current connection geometry requirements of the ASCE pre-standard. The finite element parametric analyses suggest that:

- the minimum edge distance has to be increased to $e_2 = 2.5d_0$,
- the minimum gauge for bolting can be set as $p_2 = 3.0d_0$.

These values are proposed based on the two adopted performance requirements for static loading, tensile stress and damage tolerance.

6. Summary and concluding remarks

The influence of important geometric parameters affecting the net section rupture mechanism is investigated in the stress and failure analysis carried in this paper. A comprehensive finite element parametric study is conducted for that purpose. Following a general discussion of the results, the main findings ae highlighted and their implications on composite strength are appraised with emphasis given to the proposed requirements included in the ASCE pre-standard.

At the time this research was done, there were no publicly available test results on this topic, and therefore this paper represents one of the earliest studies that have addressed the implications of geometric characteristics on net section failure in pultruded FRP bolted connection performance. It is hoped that the new knowledge and understanding presented will spur more research in this important area and provide insight that will help direct future research and code development endeavours, such as those now transforming the ASCE pre-standard into a published standard with consensus design procedures.

Acknowledgments

This paper was produced in the framework of the project *Structural joints for building frames of pultruded fibre reinforced polymers*. This research was supported by a Marie Curie Intra European Fellowship within the 7th European Community Framework Programme under contract grant PIEF-GA-2012-327142.

References

[1] Girão Coelho AM, Mottram JT. A review of the behaviour and analysis of bolted connections and joints in pultruded fibre reinforced polymers. Mater Design 2015;74:86-107.

[2] ASCE (American Society of Civil Engineers). Pre-Standard for Load & Resistance Factor Design (LFRD) of Pultruded Reinforced Polymer (FRP) Structures. 2010.

[3] Marine design manual for fiberglass reinforced plastics. Gibbs & Cox, Inc., New York: McGraw-Hill Book Company, 1960.

[4] Turvey GF, Wang P. An FE analysis of the stresses in pultruded GRP single-bolt tension joints and their implications for joint design. Compos Struct 2008;86:1014-1021.

[5] Zhou Y, Yazdani-Nezhad H, McCarthy MA, Wan X, McCarthy C. A study of intra-laminar damage in double-lap, multi-bolt, composite joints with variable clearance using continuum damage mechanics. Compos Struct 2014;116:441-452.

[6] Girão Coelho AM, Mottram JT, Harries KA. Finite element guidelines for simulation of fibre-tension dominated failures in composite materials validated by case studies. Compos Struct 2015;126:299-313.

[7] Cunningham D, Harries KA, Bell AJ. Open-hole tension capacity of pultruded GFRP having staggered hole arrangement. Eng Struct 2015;95:8-15.

[8] Eurocode 3: Design of steel structures – Part 1-8: Design of joints. *EN* 1993-1-8, Brussels: CEN (European Committee for Standardization), 2005.

[9] Pinho S, Robinson P, Iannucci I. Fracture toughness of the tensile and compressive fibre failure modes in laminated composites. Compos Sci Technol 2006;66(13):2069–2079.

[10] Maimí P, Camanho PP, Mayugo JA, Dávila CG. A continuum damage model for composite laminates, Part I: constitutive model. Mech Mater 2007;39:897-908.

[11] Abaqus [Computer Software], Version 6.13 Dassault systems, http://www.3ds.com/products-services/simulia/products/abaqus.

[12] Hashin Z, Failure criteria for unidirectional fiber composites. J Appl Mech 1980;47:329-334.

[13] Matzenmiller A, Lubliner J, Taylor RL. A constitutive model for anisotropic damage in fiber-composites. Mech Mater 1995;20:125-152.

[14] Bažant ZP, Oh BH. Crack band theory for fracture of concrete. Mater Struct 1983;16:155-177.

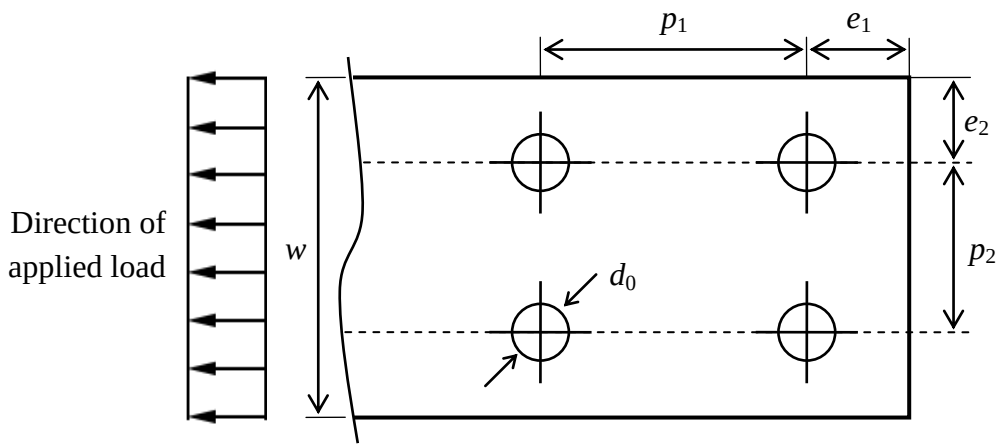

Fig. 1. Definition of the connection geometry and symbols for spacing of fasteners

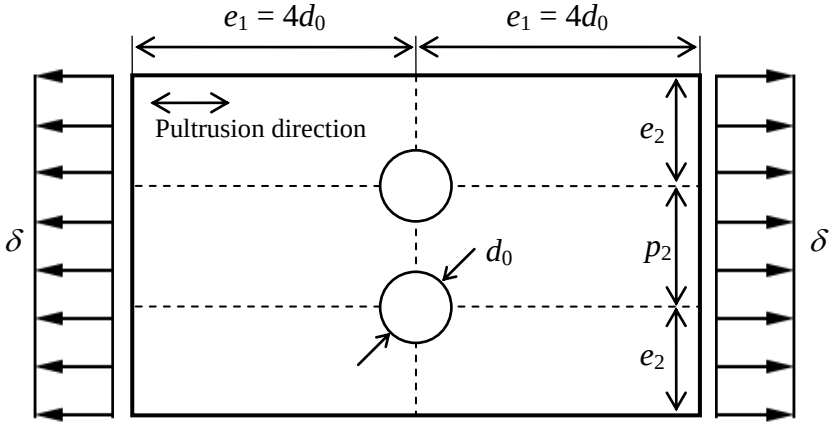

Fig. 2. Generic test configuration

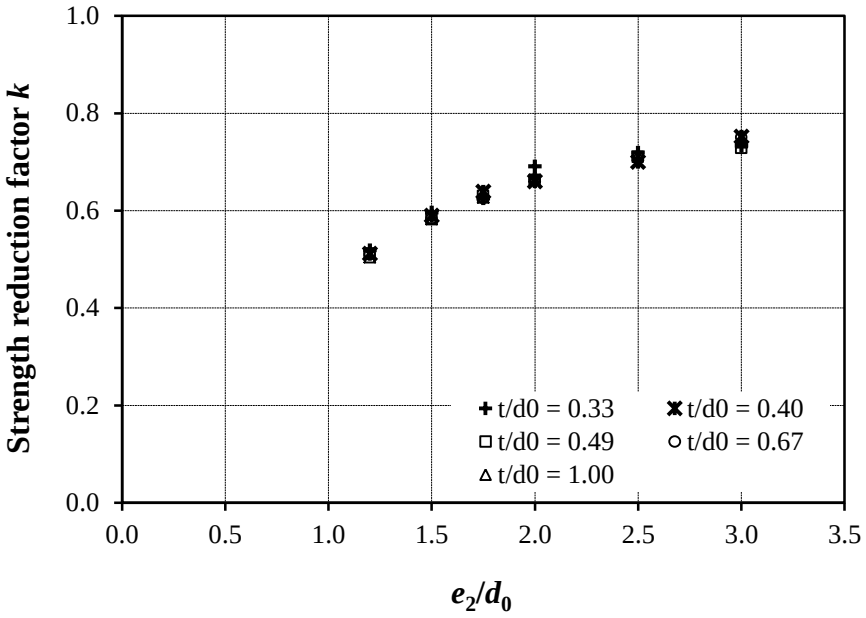

Fig. 3. Variation of edge distance to hole diameter ratio and the strength reduction factor curves with different thickness of plate to hole diameter ratio

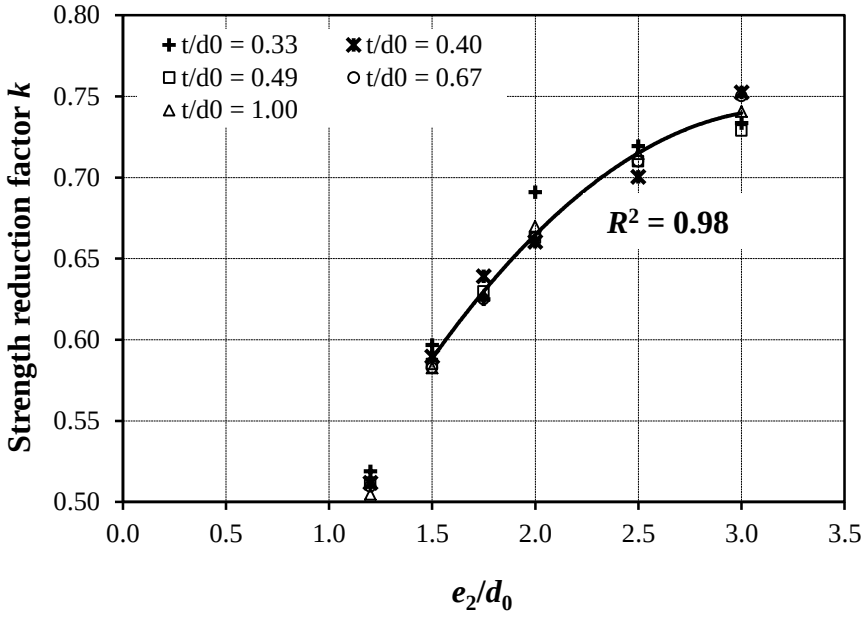

Fig. 4. Regression data analysis for the edge distance to hole diameter ratio

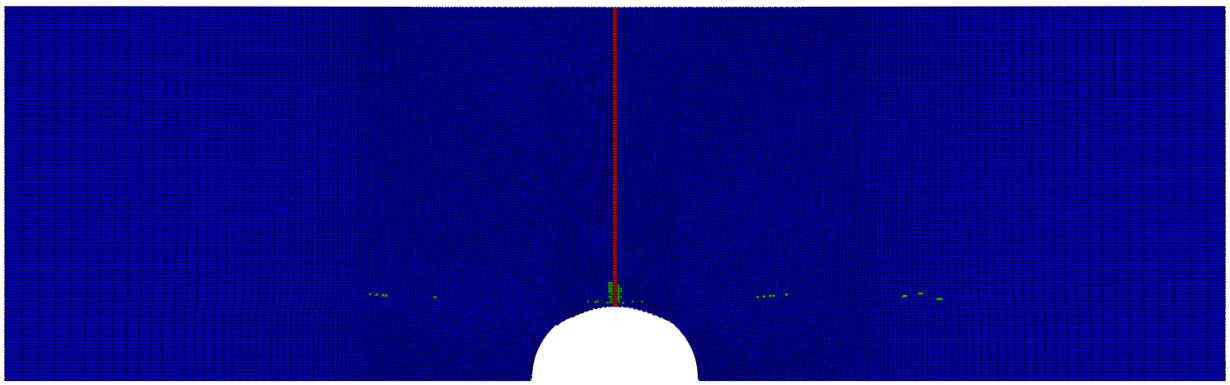

a) Full damage to the edge (σ_{Fd} = 286 MPa)

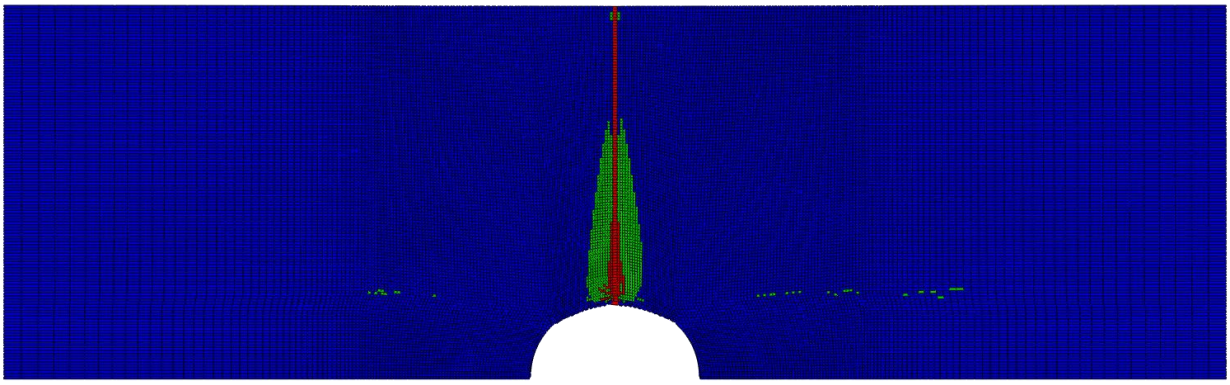

b) Maximum load (σ_{max} = 301 MPa)

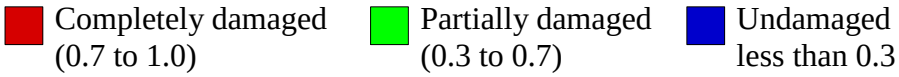

Fig. 5. Specimen E2_4.0-2.5-0-0-1/2: plot of fibre-tension damage

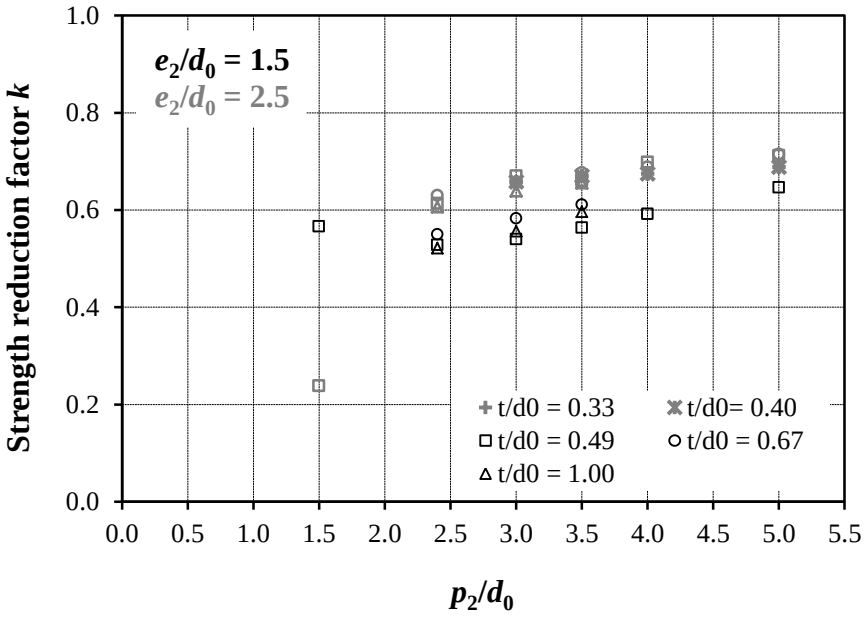

Fig. 6. Variation of gauge for the bolting to hole diameter ratio and the strength reduction factor curves with different thickness of plate to hole diameter ratio

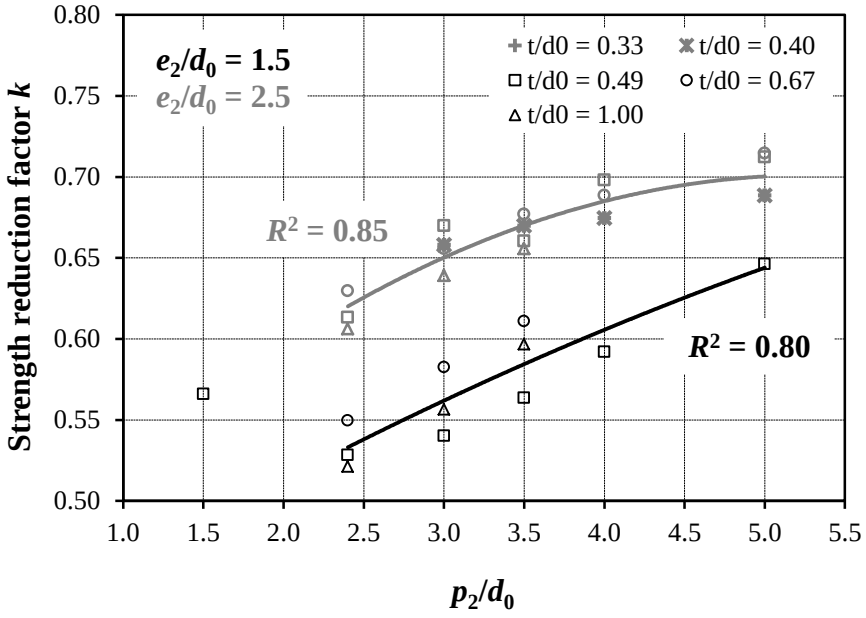

Fig. 7. Regression data analysis for the gauge for the bolting to hole diameter ratio

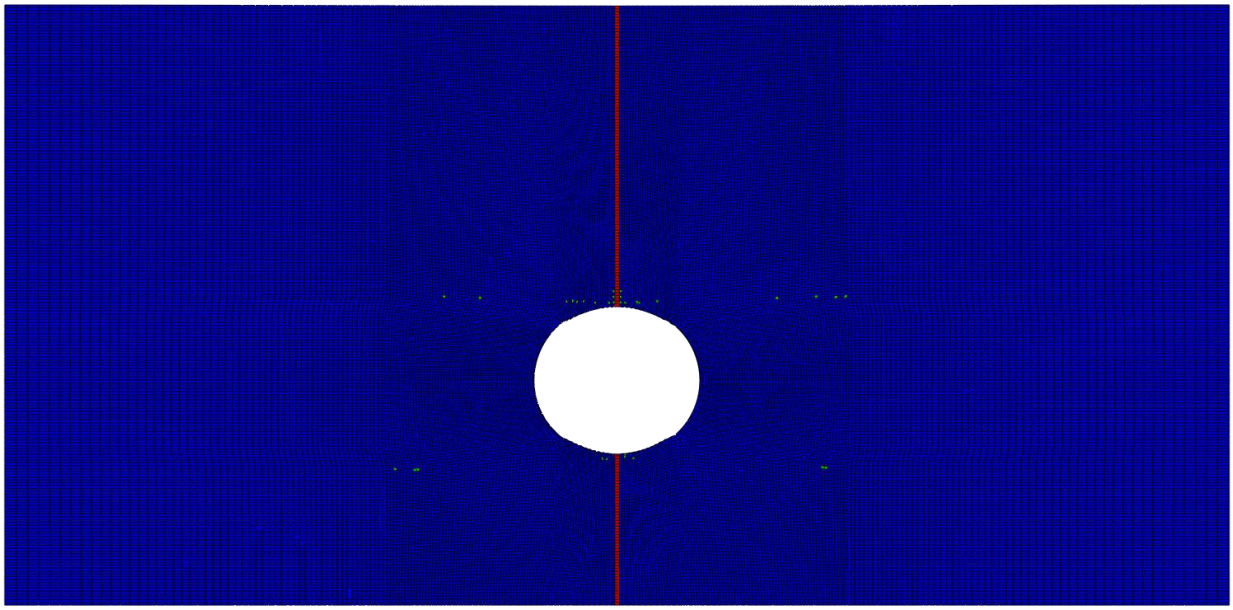

a) Full damage to the edge (σ_{Fd} = 255 MPa)

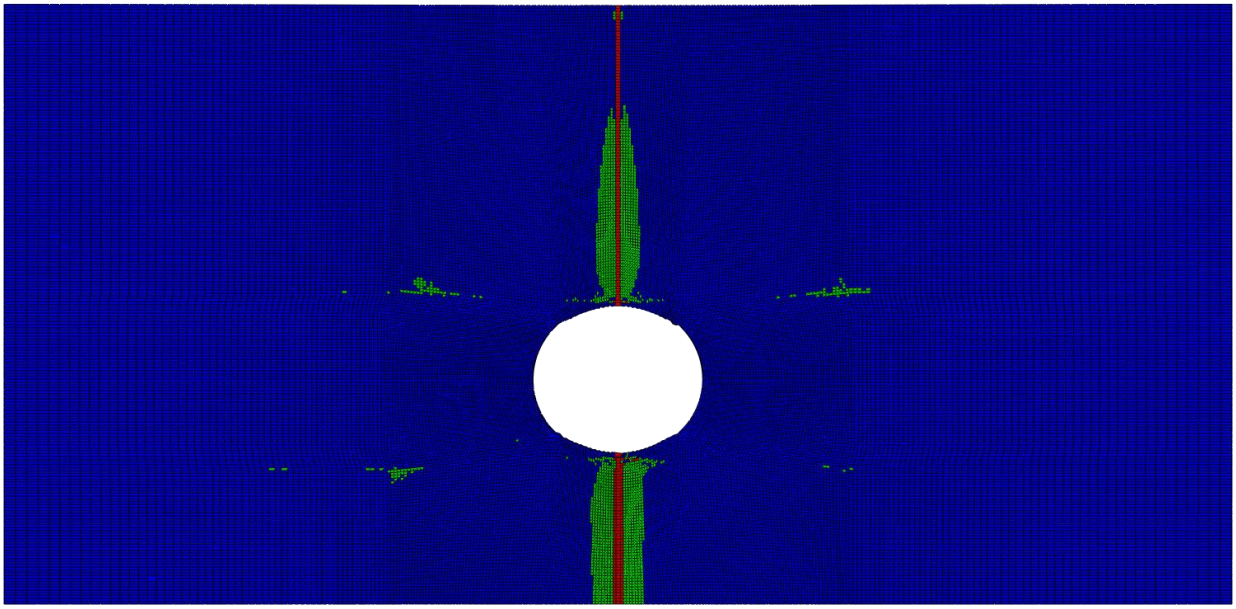

b) Maximum load (σ_{max} = 284 MPa)

Completely damaged (0.7 to 1.0)

Partially damaged (0.3 to 0.7)

Undamaged less than 0.3

Fig. 8. Specimen P2_4.0-2.5-0-3.0-1/2: plot of fibre-tension damage

Table 1. Minimum requirements for bolted connection geometries

Distances and spacings (see Fig. 1)	Pultruded connections (ASCE pre-standard)	Steel connections (EN1993-1-8)
e_1	$2d$	$1.2d_0$
e_2	$1.5d$	$1.2d_0$
p_1	$4d$	$2.2d_0$
p_2	$4d$	$2.4d_0$

Table 2. (Relevant) Material properties of the pultruded specimens

Elastic lamina properties		Lamina strength properties		Fracture toughness	
E_1 (N/mm^2)	19843	$f_{1,T}$ (N/mm^2)	424	$G_{1,T,c}$ (N/mm)	100
E_2 (N/mm^2)	6435	$f_{2,T}$ (N/mm^2)	94.5	$G_{2,T,c}$ (N/mm)	1.2

Table 3. Parametric study

Parameter	Range of parameter selected
d_0 (mm)	6.4, 9.6, 13.1, 16.0, 19.2
t/d_0	0.33, 0.40, 0.49, 0.67, 1.00
p_2/d_0	1.5, 2.4*, 3.0, 3.5, 4.0, 5.0
e_2/d_0	1.2*, 1.5, 1.75, 2.0, 2.5, 3.0

* Value adopted in EN 1993-1-8 (CEN 2005)

Table 4. Summary of finite element parametric studies: series *E*2

Test	Geometric properties					d_0	w	σ_{max}	R_{FRP}
	e_1/d_0	e_2/d_0	p_1/d_0	p_2/d_0	t/d_0	(mm)	(mm)	(MPa)	
Series E2									
E2_4.0-1.2-0-0-1/3	4.0	1.2	−	−	0.33	19.2	46.1	220	0.93
E2_4.0-1.2-0-0-1/2.5	4.0	1.2	−	−	0.40	16.0	38.4	217	0.95
E2_4.0-1.2-0-0-1/2	4.0	1.2	−	−	0.49	13.1	31.4	217	0.93
E2_4.0-1.2-0-0-2/3	4.0	1.2	−	−	0.67	9.6	23.0	216	0.92
E2_4.0-1.2-0-0-1	4.0	1.2	−	−	1.00	6.4	15.4	214	0.93
E2_4.0-1.5-0-0-1/3	4.0	1.5	−	−	0.33	19.2	57.6	253	0.94
E2_4.0-1.5-0-0-1/2.5	4.0	1.5	−	−	0.40	16.0	48.0	250	0.96
E2_4.0-1.5-0-0-1/2	4.0	1.5	−	−	0.49	13.1	39.3	248	0.95
E2_4.0-1.5-0-0-2/3	4.0	1.5	−	−	0.67	9.6	28.8	247	0.95
E2_4.0-1.5-0-0-1	4.0	1.5	−	−	1.00	6.4	19.2	247	0.93
E2_4.0-1.75-0-0-1/3	4.0	1.75	−	−	0.33	19.2	67.2	265	0.96
E2_4.0-1.75-0-0-1/2.5	4.0	1.75	−	−	0.40	16.0	56.0	271	0.94
E2_4.0-1.75-0-0-1/2	4.0	1.75	−	−	0.49	13.1	45.9	267	0.96
E2_4.0-1.75-0-0-2/3	4.0	1.75	−	−	0.67	9.6	33.6	265	0.95
E2_4.0-1.75-0-0-1	4.0	1.75	−	−	1.00	6.4	22.4	266	0.94
E2_4.0-2.0-0-0-1/3	4.0	2.0	−	−	0.33	19.2	76.8	293	0.94
E2_4.0-2.0-0-0-1/2.5	4.0	2.0	−	−	0.40	16.0	64.0	280	0.98
E2_4.0-2.0-0-0-1/2	4.0	2.0	−	−	0.49	13.1	52.4	281	0.96
E2_4.0-2.0-0-0-2/3	4.0	2.0	−	−	0.67	9.6	38.4	281	0.94
E2_4.0-2.0-0-0-1	4.0	2.0	−	−	1.00	6.4	25.6	284	0.94
E2_4.0-2.5-0-0-1/3	4.0	2.5	−	−	0.33	19.2	96.0	305	0.94
E2_4.0-2.5-0-0-1/2.5	4.0	2.5	−	−	0.40	16.0	80.0	297	0.98
E2_4.0-2.5-0-0-1/2	4.0	2.5	−	−	0.49	13.1	65.5	301	0.95
E2_4.0-2.5-0-0-2/3	4.0	2.5	−	−	0.67	9.6	48.0	301	0.94
E2_4.0-2.5-0-0-1	4.0	2.5	−	−	1.00	6.4	32.0	303	0.96
E2_4.0-3.0-0-0-1/3	4.0	3.0	−	−	0.33	19.2	115.2	311	0.96
E2_4.0-3.0-0-0-1/2.5	4.0	3.0	−	−	0.40	16.0	96.0	319	0.94
E2_4.0-3.0-0-0-1/2	4.0	3.0	−	−	0.49	13.1	78.6	309	0.97
E2_4.0-3.0-0-0-2/3	4.0	3.0	−	−	0.67	9.6	57.6	318	0.93
E2_4.0-3.0-0-0-1	4.0	3.0	−	−	1.00	6.4	38.4	314	0.95

Table 5. Summary of finite element parametric studies: series *P*2

Test	Geometric properties					d_0	w	σ_{max}	R_{FRP}
	e_1/d_0	e_2/d_0	p_1/d_0	p_2/d_0	t/d_0	(mm)	(mm)	(MPa)	
Series P2									
P2_4.0-1.5-0-1.5-1/2	4.0	1.5	−	1.5	0.49	13.1	58.9	240	0.90
P2_4.0-2.5-0-1.5-1/2	4.0	2.5	−	1.5	0.49	13.1	85.2	101	0.88
P2_4.0-1.5-0-2.4-1/2	4.0	1.5	−	2.4	0.49	13.1	70.7	224	0.94
P2_4.0-1.5-0-2.4-2/3	4.0	1.5	−	2.4	0.67	9.6	51.8	233	0.91
P2_4.0-1.5-0-2.4-1	4.0	1.5	−	2.4	1.00	6.4	34.6	221	0.92
P2_4.0-2.5-0-2.4-1/2	4.0	2.5	−	2.4	0.49	13.1	96.9	260	0.89
P2_4.0-2.5-0-2.4-2/3	4.0	2.5	−	2.4	0.67	9.6	71.0	267	0.88
P2_4.0-2.5-0-2.4-1	4.0	2.5	−	2.4	1.00	6.4	47.4	257	0.92
P2_4.0-1.5-0-3.0-1/2	4.0	1.5	−	3.0	0.49	13.1	78.6	229	0.91
P2_4.0-1.5-0-3.0-2/3	4.0	1.5	−	3.0	0.67	9.6	57.6	247	0.93
P2_4.0-1.5-0-3.0-1	4.0	1.5	−	3.0	1.00	6.4	38.4	236	0.97
P2_4.0-2.5-0-3.0-1/3	4.0	2.5	−	3.0	0.33	19.2	153.6	279	0.92
P2_4.0-2.5-0-3.0-1/2.5	4.0	2.5	−	3.0	0.40	16.0	128.0	283	0.91
P2_4.0-2.5-0-3.0-1/2	4.0	2.5	−	3.0	0.49	13.1	104.8	284	0.90
P2_4.0-2.5-0-3.0-2/3	4.0	2.5	−	3.0	0.67	9.6	76.8	278	0.90
P2_4.0-2.5-0-3.0-1	4.0	2.5	−	3.0	1.00	6.4	51.2	271	0.91
P2_4.0-1.5-0-3.5-1/2	4.0	1.5	−	3.5	0.49	13.1	85.2	239	0.93
P2_4.0-1.5-0-3.5-2/3	4.0	1.5	−	3.5	0.67	9.6	62.4	259	0.91
P2_4.0-1.5-0-3.5-1	4.0	1.5	−	3.5	1.00	6.4	41.6	253	0.95
P2_4.0-2.5-0-3.5-1/3	4.0	2.5	−	3.5	0.33	19.2	163.2	284	0.93
P2_4.0-2.5-0-3.5-1/2.5	4.0	2.5	−	3.5	0.40	16.0	136.0	286	0.92
P2_4.0-2.5-0-3.5-1/2	4.0	2.5	−	3.5	0.49	13.1	111.4	280	0.89
P2_4.0-2.5-0-3.5-2/3	4.0	2.5	−	3.5	0.67	9.6	81.6	287	0.90
P2_4.0-2.5-0-3.5-1	4.0	2.5	−	3.5	1.00	6.4	54.4	278	0.94
P2_4.0-1.5-0-4.0-1/2	4.0	1.5	−	4.0	0.49	13.1	91.7	251	1.00
P2_4.0-2.5-0-4.0-1/3	4.0	2.5	−	4.0	0.33	19.2	172.8	286	0.94
P2_4.0-2.5-0-4.0-1/2.5	4.0	2.5	−	4.0	0.40	16.0	144.0	288	0.91
P2_4.0-2.5-0-4.0-1/2	4.0	2.5	−	4.0	0.49	13.1	117.9	296	0.89
P2_4.0-2.5-0-4.0-2/3	4.0	2.5	−	4.0	0.67	9.6	86.4	292	0.91
P2_4.0-1.5-0-5.0-1/2	4.0	1.5	−	5.0	0.49	13.1	104.8	274	0.97
P2_4.0-2.5-0-5.0-1/3	4.0	2.5	−	5.0	0.33	19.2	192.0	292	0.95
P2_4.0-2.5-0-5.0-1/2.5	4.0	2.5	−	5.0	0.40	16.0	160.0	301	0.95
P2_4.0-2.5-0-5.0-1/2	4.0	2.5	−	5.0	0.49	13.1	131.0	302	0.90
P2_4.0-2.5-0-5.0-2/3	4.0	2.5	−	5.0	0.67	9.6	96.0	303	0.90